

AttriCtrl: Fine-Grained Control of Aesthetic Attribute Intensity in Diffusion Models

Die Chen¹, Zhongjie Duan², Zhiwen Li¹, Cen Chen¹, Daoyuan Chen², Yaliang Li², Yinda Chen²

¹East China Normal University

²Alibaba Group

{dchen, zhiwenli}@stu.ecnu.edu.cn, cenchen@dase.ecnu.edu.cn,

{duanzhongjie.dzj, daoyuan.chen.cdy, yaliang.li, yingda.chen}@alibaba-inc.com

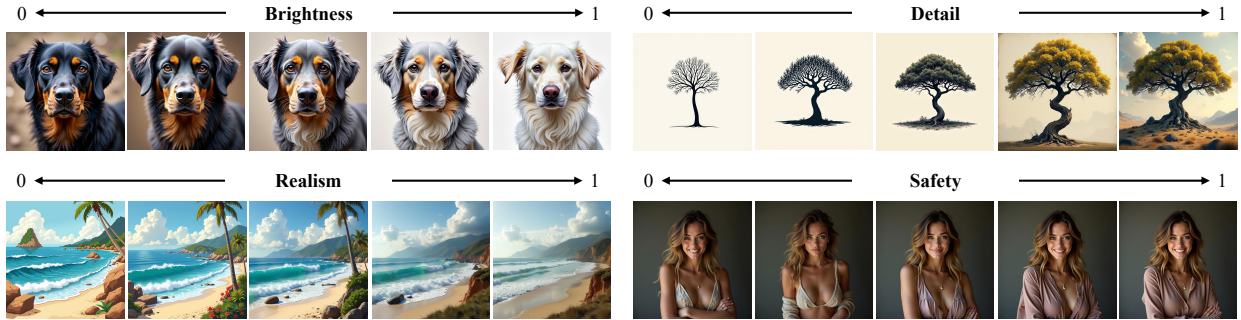


Figure 1: Overview. Our proposed AttriCtrl enables fine-grained control over aesthetic attributes by modulating their intensity in the generated image. Given a scalar value in $[0, 1]$ for each attribute, our method achieves continuous and precise control over brightness, realism, detail, and safety, allowing intuitive customization of visual content.

Abstract

Recent breakthroughs in text-to-image diffusion models have significantly enhanced both the visual fidelity and semantic controllability of generated images. However, fine-grained control over aesthetic attributes remains challenging, especially when users require continuous and intensity-specific adjustments. Existing approaches often rely on vague textual prompts, which are inherently ambiguous in expressing both the aesthetic semantics and the desired intensity, or depend on costly human preference data for alignment, limiting their scalability and practicality. To address these limitations, we propose AttriCtrl, a plug-and-play framework for precise and continuous control of aesthetic attributes. Specifically, we quantify abstract aesthetics by leveraging semantic similarity from pre-trained vision-language models, and employ a lightweight value encoder that maps scalar intensities in $[0, 1]$ to learnable embeddings within diffusion-based generation. This design enables intuitive and customizable aesthetic manipulation, with minimal training overhead and seamless integration into existing generation pipelines. Extensive experiments demonstrate that AttriCtrl achieves accurate control over individual attributes as well as flexible multi-attribute composition. Moreover, it is fully compatible with popular open-source controllable generation frameworks, showcasing strong integration capability and practical utility across diverse generation scenarios.

Introduction

With the emergence of large-scale pretrained diffusion models (Ramesh et al. 2022; Podell et al. 2023; Nichol et al. 2021), text-to-image generation has made significant strides in both semantic understanding and high-quality visual synthesis (Sohl-Dickstein et al. 2015; Ho, Jain, and Abbeel 2020; Zhang, Rao, and Agrawala 2023; Hertz et al. 2022; Ye et al. 2023; Mou et al. 2024). Despite this progress, current models still struggle to align with human aesthetic perception in a fine-grained manner, limiting their applicability in real-world creative and user-facing scenarios.

A major challenge stems from the inherently subjective and dynamic nature of aesthetic preferences. Judgments on aesthetics not only vary across individuals but also fluctuate within the same user based on context, emotion, or task. This makes aligning model outputs with human preferences fundamentally uncertain and fluid, posing considerable obstacles for model design and training. Additionally, the limited expressiveness of current text encoders (Raffel et al. 2020; Radford et al. 2021) hampers the effectiveness of prompt-based control. Instructions such as “*more intricate details*” or “*brighter colors*” are often too ambiguous, and models struggle to interpret comparative or gradable expressions like “*more*”, “*less*”, or “*slightly*”, resulting in unreliable or inconsistent control over aesthetic outcomes.

This leads to a central research question: how can we sys-

tematically quantify aesthetic attributes and design a controllable generation mechanism that flexibly accommodates diverse user preferences and contexts? For instance, content designed for children may call for lower realism and detail to resemble picture book illustrations, whereas artistic exploration may demand highly detailed and visually striking outputs. Personalized generation thus requires the model to understand both the intensity and specific visual expressions of multiple aesthetic attributes.

Recent work has explored preference alignment using feedback-based methods. Reinforcement learning (Kirstain et al. 2023; Liang et al. 2024) and direct preference optimization (Fan et al. 2023; Wallace et al. 2024) leverage human-labeled data to train reward models that guide generation toward preferred outcomes. While such methods have shown promising improvements in generation quality, they typically rely on large-scale, high-quality annotations and are computationally intensive, limiting scalability and practicality. Alternative efforts have sought to improve model architecture by integrating attention mechanisms (Wu et al. 2024) or modular components to better capture preference signals (Si et al. 2024). However, the above works often assume a single optimal preference target and overlook the fluid, multi-faceted nature of aesthetic judgment. Moreover, they lack mechanisms for precise modeling of how specific aesthetic attributes influence the output, thereby failing to offer fine-grained controllability in complex use cases.

To address these limitations, we propose a two-fold solution: (1) a quantitative modeling scheme for aesthetic attributes, and (2) a controllable generation mechanism for personalized image synthesis. To quantify these diverse attributes, we introduce a tailored quantification strategy that combines direct metrics and vision-language model-based semantic similarity, enabling effective modeling of both concrete and abstract aesthetic attributes. Building on this, we present AttriCtrl, a plug-and-play adapter designed to control the intensity of aesthetic attributes. AttriCtrl incorporates a lightweight value encoder that maps user-specified scalar intensity values to semantically meaningful embeddings. The adapter is trained on curated subsets from large-scale image corpora, while the base diffusion model remains frozen, ensuring low computational overhead and easy integration. During inference, the adapter modulates generation behavior based on these embeddings, enabling flexible control over individual or composite aesthetic preferences. Extensive experiments demonstrate that AttriCtrl supports accurate and interpretable control over multiple attributes and improves output diversity. Furthermore, it is compatible with widely adopted controllable generation frameworks such as ControlNet (Zhang, Rao, and Agrawala 2023), InfiniteYou (Jiang et al. 2025), highlighting its versatility and potential for real-world deployment.

Our key contributions are summarized as follows:

- We address the underexplored problem of fine-grained, intensity-controllable aesthetic attribute manipulation in diffusion-based image generation.
- We develop a hybrid quantification strategy combining metric-based analysis and semantic similarity to model

both concrete and abstract aesthetic attributes.

- We propose AttriCtrl, a lightweight, plug-and-play adapter that enables precise, compositional control over aesthetics and integrates seamlessly with existing controllable generation frameworks.

Related Work

Diffusion Models Diffusion models have emerged as a dominant paradigm in image generation due to their stable training dynamics and strong generative performance (Nichol et al. 2021; Sohl-Dickstein et al. 2015; Ho, Jain, and Abbeel 2020). With the advent of large-scale datasets and increasing computational power (Rombach et al. 2022; Schuhmann et al. 2022), diffusion-based methods have rapidly become the foundation of modern image synthesis. Several representative models have significantly influenced both academic and industrial applications. For instance, DALL-E (Ramesh et al. 2021), proposed by OpenAI, combines diffusion mechanisms with powerful language understanding to achieve high-quality text-to-image generation. Stable Diffusion (Podell et al. 2023), developed by Stability AI, gained widespread adoption due to its open-source nature, enabling diverse downstream tasks and extensive customization. More recently, the FLUX (Labs 2025) model has demonstrated a strong trade-off among generation speed, diversity, and controllability, making it well-suited for practical deployment scenarios.

Controllable Generation Controllable generation is a key research direction in the recent advancement of diffusion models. It focuses on enabling users to exert greater influence and customization over the generation process. A wide range of control inputs have been explored, including depth maps, sketches, paint strokes and reference photo collections (Voynov, Aberman, and Cohen-Or 2023; Meng et al. 2021; Kumari et al. 2023; Ruiz et al. 2023; Xiao et al. 2025). These inputs provide additional guidance signals that help steer the model toward outputs that better align with user intentions. In parallel, several works have investigated modifications to model architecture to enhance controllability. Methods such as Prompt-to-Prompt (Hertz et al. 2022), P+ (Voynov et al. 2023), and IP-Adapter (Ye et al. 2023) focus on manipulating the cross-attention modules to achieve more precise control over image semantics and style. Among the most representative solutions, ControlNet (Zhang, Rao, and Agrawala 2023) and T2I-Adapter (Mou et al. 2024) introduce external modules that can be attached to pretrained diffusion models without altering their original parameters. Furthermore, instruction-based editing approaches, such as InstructPix2Pix (Brooks, Holynski, and Efros 2023) and EMU-Edit (Sheynin et al. 2024), allow users to edit existing images by providing natural language instructions, which improves both usability and flexibility in controllable generation tasks.

Aesthetic Modeling Modeling aesthetics in image generation has gained increasing attention, as user expectations evolve from mere photorealism to subjective and nuanced visual preferences. Early methods relied on handcrafted fea-

tures or rule-based heuristics to assess aesthetic quality, but these approaches struggle to capture the complexity of human perception (Celona et al. 2022). Recent works have explored improving aesthetic quality either by architectural enhancement or preference alignment. For example, FreeU (Si et al. 2024) enhances U-Net structures in diffusion models to preserve high-frequency details and visual quality with no extra cost. VMix (Wu et al. 2024) introduces a cross-attention mixing strategy to control aesthetic attributes such as lighting and detail levels, offering interpretable and flexible generation. On the preference alignment side, methods like DPOK (Fan et al. 2023) and Diffusion-DPO (Wallace et al. 2024) adapt direct preference optimization to fine-tune diffusion models based on human feedback. These approaches improve subjective image quality by learning from pairwise comparisons, but often require costly human annotation and do not explicitly disentangle fine-grained aesthetic factors. While promising, most existing methods either assume a static aesthetic goal or lack mechanisms for precise control over individual visual attributes. This highlights the need for more structured and controllable aesthetic modeling in diffusion frameworks.

Method

To achieve precise and continuous control over aesthetic attributes, we formulate the problem in two stages: (1) represent the intensity of a given aesthetic attribute in an image as a normalized scalar value in the range $[0, 1]$; (2) use this scalar value to guide diffusion-based image generation with the corresponding intensity of the desired attribute. We elaborate on these two components below.

Aesthetic Attribute Quantification

We define four aesthetic attributes relevant to human preference and responsible generation: *brightness*, *detail*, *realism*, and *safety*. Notably, the safety attribute supports tiered control, enabling appropriate content filtering for users across different age groups. While our framework allows flexible adjustment of safety intensity, we recommend that system administrators set this value to its maximum during deployment to ensure default content appropriateness. Access to modify this parameter should be restricted from general users to prevent unintended exposure to unsafe content.

To quantify these attributes, we adopt a hybrid strategy: for concrete attributes (*brightness* and *detail*), we employ direct metric-based estimation; for more abstract, semantic attributes (*realism* and *safety*), we leverage pretrained vision-language models to compute cross-modal similarity between images and descriptive text prompts. Representative examples of the quantified values are shown in Figure 2.

Direct Estimation Two attributes—*brightness* and *detail*—can be directly quantified using well-established computational metrics.

Brightness is estimated in the HSV (Hue, Saturation, Value) color space. Specifically, we extract the Value channel, which directly corresponds to perceived brightness, and compute its mean pixel intensity normalized by 255—the maximum possible value in 8-bit encoding. This yields a raw

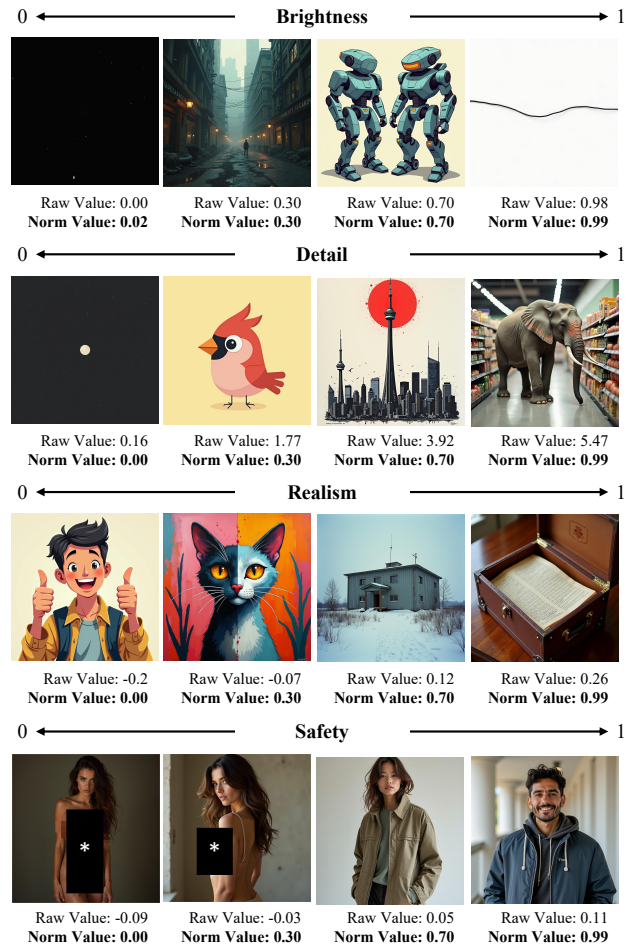


Figure 2: Examples of aesthetic attribute intensities in the training dataset. We show the raw values computed via quantitative metrics and the normalized values after value mapping, scaled to the $[0, 1]$ range for consistent control.

value of the brightness attribute in the range $[0, 1]$, where 0 indicates complete darkness and 1 indicates maximum brightness. Formally, for an image I , the brightness intensity value is defined as:

$$Brightness(I) = \frac{1}{H \cdot W} \sum_{i=1}^h \sum_{j=1}^w \frac{v_{i,j}}{255}, \quad (1)$$

where $v_{i,j}$ denotes the value channel of the pixel (i, j) in the HSV representation, and H, W are the height and width of the image, respectively.

For **detail**, we measure visual complexity through the Shannon entropy of the image’s grayscale intensity distribution. First, the image is converted to grayscale to eliminate chromatic variations and emphasize structural content. A histogram over 256 levels is computed and normalized into a probability distribution. The raw value of the detail intensity is then given by the entropy of this distribution:

$$Detail(I) = Entropy(Hist(I)) = - \sum_{k=1}^{256} p_k \log(p_k), \quad (2)$$

where p_k denotes the probability of the k -th grayscale intensity level in image I . The resulting value lies in the range $[0, \log(256)]$, with higher values indicating a more complex grayscale distribution and richer visual details.

Similarity-Based Estimation For abstract aesthetic attributes such as *realism* and *safety*, direct quantification is inherently difficult due to their reliance on high-level semantic understanding and contextual interpretation. To address this challenge, we leverage the multimodal representation capabilities of pretrained vision-language models—specifically CLIP (openai 2022)—which encode both images and text into a shared embedding space. We compute the cosine similarity between an image embedding e_I and a set of carefully crafted textual prompts that describe the target attribute, using the resulting value as a proxy for the attribute’s intensity. The similarity is defined as:

$$\text{sim}(e_I, e_T) = \frac{e_I \cdot e_T}{\|e_I\| \cdot \|e_T\|}. \quad (3)$$

To quantify **realism**, we construct a pair of contrastive prompts that describe the two ends of the realism spectrum. The positive prompt is “*a real photograph, realistic details and natural lighting*”, representing natural photographic scenes, while the negative prompt is “*a cartoon image, a human-created artistic representation, such as an illustration or painting*”, which captures stylized or artificial depictions. We encode these prompts into text embeddings e_{pos} and e_{neg} using CLIP’s text encoder and obtain the image embedding e_I via the image encoder. The realism intensity value is defined as:

$$\text{Realism}(I) = \text{sim}(e_I, e_{\text{pos}}) - \text{sim}(e_I, e_{\text{neg}}), \quad (4)$$

where higher values indicate stronger semantic alignment with realistic photographic content.

For **safety**, defining a comprehensive positive description of safe content is inherently challenging, as safety is typically characterized not by what is present, but by what is absent. Instead of attempting to exhaustively enumerate all forms of acceptable or safe imagery, we leverage the well-defined and widely adopted notions of unsafe content encoded in existing automated safety checkers (CompVis 2022). Specifically, we use a pretrained textual embedding e_s representing unsafe content and compute its cosine similarity with the image embedding e_I as:

$$\text{Safety}(I) = -(\text{sim}(e_I, e_s) - t), \quad (5)$$

where the threshold t defines the maximum allowable similarity before the image is classified as unsafe. To ensure consistency with the directionality of other aesthetic attributes, we invert the value such that higher values indicate greater perceived safety.

Value Mapping To enable consistent and comparable control over all aesthetic attributes during generation, we normalize their raw values into a unified $[0, 1]$ range. This normalization ensures that different attributes—whether derived from pixel statistics or semantic similarities—are aligned on the same scale, facilitating joint modeling and intuitive user control.

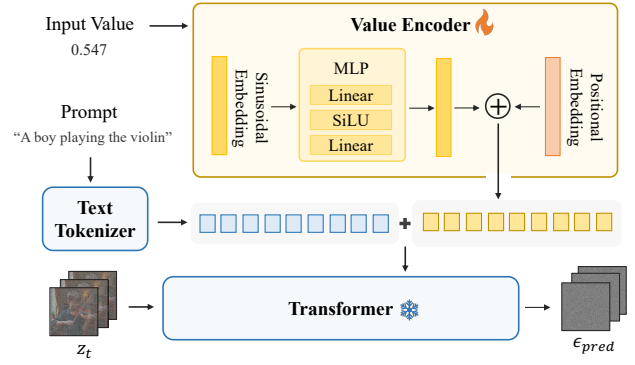


Figure 3: Framework of AttriCtrl. AttriCtrl trains a value encoder that maps a normalized attribute intensity to a multi-scale representation. The value is first sinusoidally encoded, then processed by an MLP and added to learnable position embeddings. The resulting features are concatenated with text prompts and injected into the DiT.

We employ quantile-based normalization to preserve the ordinal structure of the original distributions while achieving approximate uniformity. Specifically, for each aesthetic attribute, we divide its value range across all images into 10 equal-width bins based on the empirical minimum and maximum of the dataset. To mitigate data imbalance and avoid model bias toward specific values, we adopt a balanced sampling strategy: underpopulated bins are over-sampled with replacement, while overpopulated bins are randomly down-sampled without replacement. This yields an equal number of training samples in each bin. We then normalize the re-sampled attribute values using a rank-based transformation. For each value x_i , we compute its average rank $_i$ among all n samples, accounting for possible ties by assigning their mean rank. The normalized value is obtained as:

$$\text{normalized}_i = \frac{\text{rank}_i - 0.5}{n}, \quad (6)$$

which ensures that the normalized values are approximately uniformly distributed in $[0, 1]$.

Tailored Aesthetic Control

Preliminaries Diffusion models learn to generate images by modeling the denoising process of a latent variable corrupted by Gaussian noise. Given an input image I , it is first encoded by a variational encoder E into a latent representation $z = E(I)$. During training, Gaussian noise is progressively added to z over T timesteps, producing a noisy latent z_t at each step. A denoising network ε_θ is then trained to predict the added noise, enabling the model to gradually reconstruct the original image from pure noise. For text-to-image generation, a text prompt p is encoded into a contextual embedding c using a text encoder. This embedding is integrated into the denoising process via attention modules, allowing the model to align image synthesis with the semantics of the prompt. After denoising, the latent is passed through a decoder to reconstruct the final image.

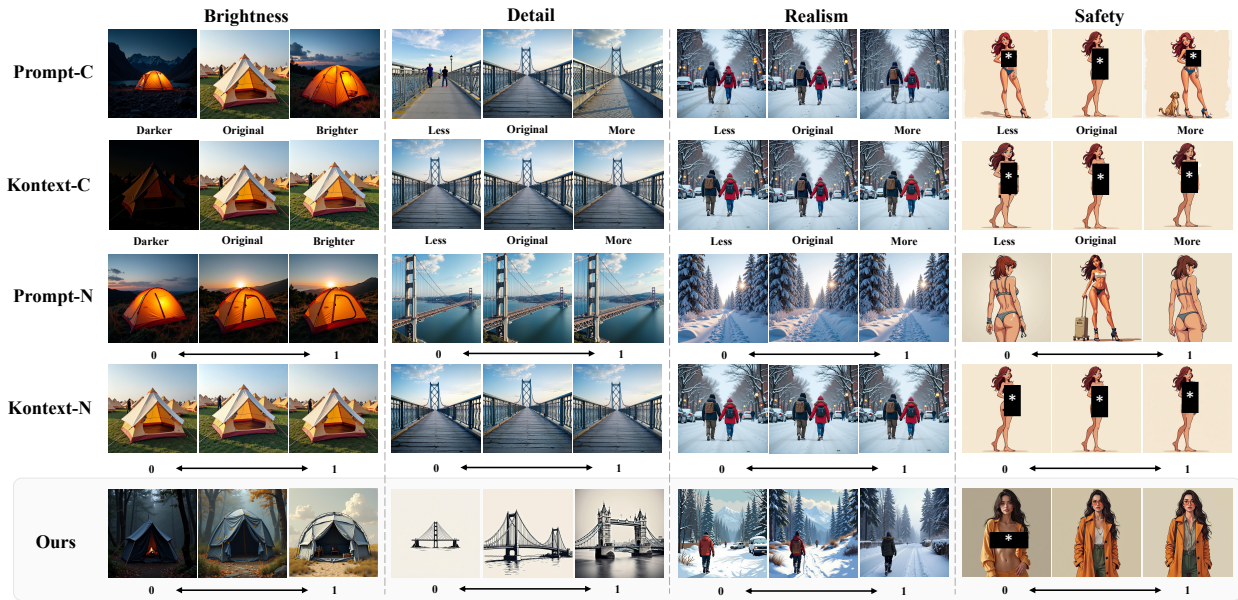


Figure 4: Qualitative comparison of different control methods. The first two rows show results using comparative textual control via prompt injection and Kontext-based editing, respectively. Rows three and four present results using numerical textual control with the same paradigms. The fifth row demonstrates the output of our proposed AttriCtrl, achieving precise attribute control.

Value Encoder As illustrated in Figure 3, we design an independent value encoder to transform the normalized intensity value into a learnable token sequence for each aesthetic attribute. Specifically, the encoding begins with a sinusoidal embedding mechanism, originally used for timestep encoding in diffusion models. Its smooth interpolation properties make it well-suited for converting continuous aesthetic values into structured high-dimensional vectors. The resulting embedding is passed through a two-layer multilayer perceptron (MLP) with SiLU activations and becomes a hidden representation, which is then duplicated and expanded into a fixed-length sequence of 32 tokens. To distinguish each token’s position within the sequence, we add a learnable positional embedding to the repeated representations. This positional encoding enables the model to assign different semantics to each token, even though they originate from the same scalar input. As a result, the encoder can capture richer attribute-specific information, which facilitates more expressive and fine-grained control during generation.

The final aesthetic intensity embedding v is concatenated along the sequence dimension of the text embedding c , forming a joint representation that enters the backbone of the diffusion model. The training objective becomes:

$$\mathcal{L}(\theta) = \mathbb{E}_{z_t, \varepsilon, c, t} \left[\|\varepsilon - \hat{\varepsilon}_\theta(z_t, c, v, t)\|_2^2 \right]. \quad (7)$$

The design of value encoder allows aesthetic control information to be seamlessly integrated, providing strong compatibility and extensibility for downstream tasks.

Multi-Attribute Composition A straightforward approach to multi-attribute aesthetic control is to merge single-attribute datasets and jointly train value encoders for all at-

tributes. However, this often results in data imbalance across attributes, hindering training stability and convergence.

To address this, we adopt a modular strategy: each aesthetic attribute is first encoded independently using its corresponding value encoder trained on single-attribute data. At inference time, the resulting embeddings are concatenated in sequence and appended to the text embedding. This composite embedding enables joint conditioning on multiple aesthetic dimensions within a unified framework.

Such a modular design leverages the composability of independently trained value encoders, allowing for flexible, plug-and-play integration of aesthetic attributes while minimizing mutual interference.

Experiments

In this section, we present systematic experiments to evaluate the effectiveness of AttriCtrl across multiple aesthetic attributes, as well as its compatibility with existing controllable generation frameworks. Additional ablation studies are provided in Appendix.

Experimental Setup

Implementation Details We use FLUX (Labs 2025) as the base model and integrate it with our value encoder module. The model is trained for 200K steps using the AdamW optimizer with a fixed learning rate of 1×10^{-5} .

Datasets For the attributes brightness, realism, and detail, we train on the first 155K samples of the EliGen (Zhang et al. 2025), a high-quality image-text dataset characterized by rich semantic diversity. For the safety, we construct a dedicated dataset to train the corresponding value encoder: 50K unsafe images are generated using adversarial prompts from

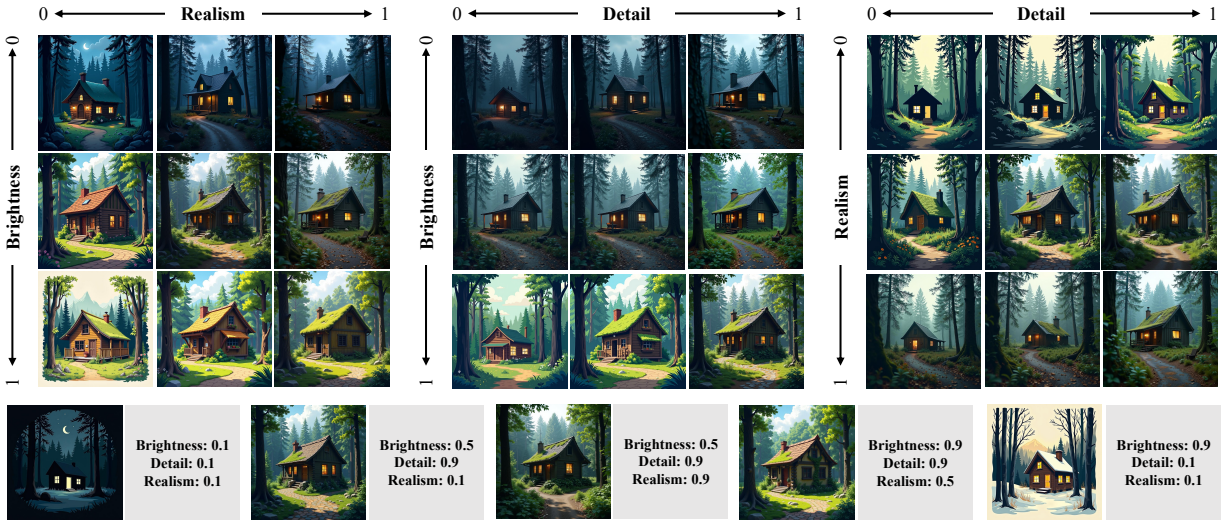


Figure 5: Qualitative results of multi-attribute control. We generate images by jointly varying combinations of attribute intensity values in a coordinated manner.

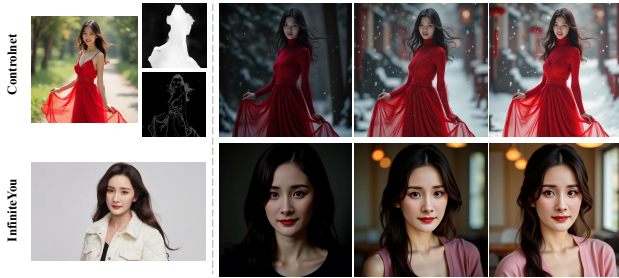


Figure 6: Compatibility of AttriCtrl with mainstream control frameworks.

RAB (Tsai et al. 2023), while 50K safe images are generated using the neutral prompt “A person wearing clothes.” We divide the raw value range into 10 equal-width bins to discretize attribute intensity levels. To mitigate distributional bias, we balance the dataset via resampling, resulting in exactly 10K samples per bin.

Baselines We systematically explore two mainstream control paradigms as baselines: (1) direct injection of control text into the prompt; and (2) post-generation instruction-based editing using external tools, we adopt Kontext (Batifol et al. 2025) in the following experiments. These two paradigms respectively represent the typical paths of control at generation and post-hoc adjustment, which are widely adopted in current controllable image generation research. Each paradigm can be further categorized based on the following form of the control text:

- Comparative textual control (C): descriptive phrases such as “Add more details” or “Make it brighter”, which rely on the model’s ability to interpret relative semantics in natural language.
- Numerical textual control (N): quantitative expressions

like “with 30% brightness” or “detail intensity: 0.7”, aiming to specify the desired attribute intensity through explicit numerical guidance.

Combining both dimensions yields four representative baseline methods. Detailed configurations of all baselines are provided in Appendix.

Qualitative Analyses

Single-attribute Control As shown in Figure 4, we compare generated results across the four attributes. Across all baselines, image variations remain minimal and lack clear visual gradation. Especially for detail and realism, most methods produce nearly identical images, indicating an ineffective activation of internal control mechanisms. Although prompt-based baselines show some distinguishability in brightness and safety, the changes are discrete and fail to match the intended intensity accurately, suggesting that models still rely on loose associations. In contrast, our AttriCtrl accurately modulates image content based on the input intensity value. For example, in the detail attribute, images progressively exhibit enhanced local complexity as the intensity value increases from 0 to 1. For safety, increasing intensity value leads to systematic suppression of inappropriate content while preserving the subject’s structure. This smooth control behavior validates the effectiveness of AttriCtrl in fine-grained attribute control. More examples are shown in Figure 7.

Multi-attribute Control We further visualize the results of multi-attribute joint control in Figure 5, demonstrating the flexibility of AttriCtrl in complex generation scenarios. Specifically, we simultaneously modulate brightness, detail, and realism to produce highly customized outputs. Experimental results show that most attribute controls are disentangled, function independently, and exhibit smooth trends that align with target intensity values. However, we observe

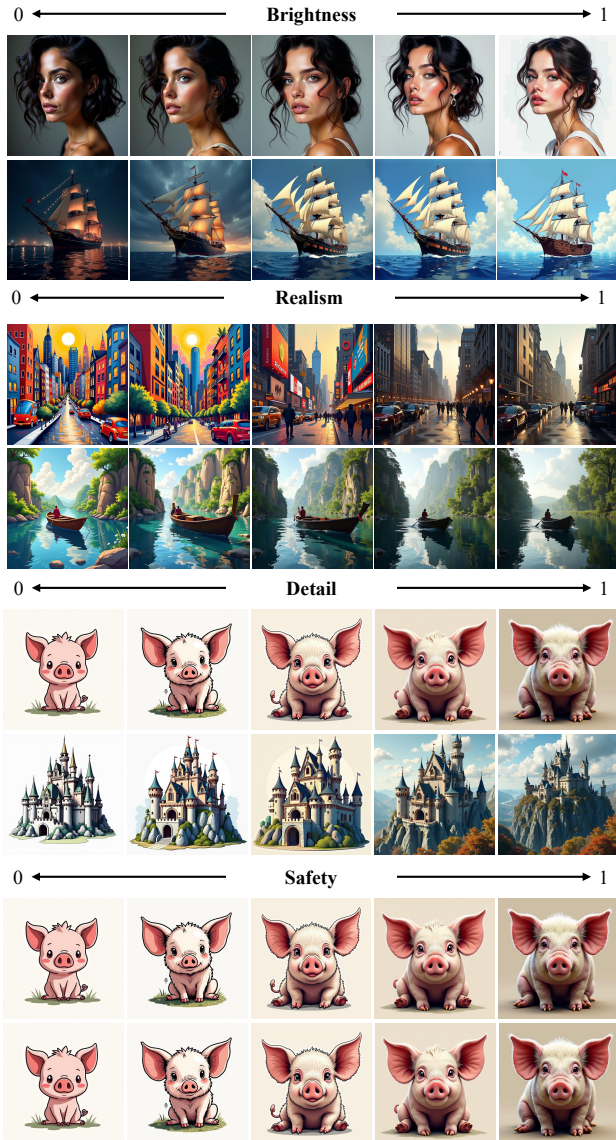


Figure 7: More examples of single attribute intensity control.

a mild coupling between realism and detail: images with higher realism intensity value tend to exhibit moderately enhanced detail, likely due to the natural correlation between photographic appearance and textural richness in training data.

User Study To further assess the perceptual quality of attribute control, we conduct a user study under a double-blind setup (details in Appendix). In each trial, participants are presented with five image sequences, which are generated from the same base prompt with progressively increasing target intensity, corresponding to four baseline methods and our proposed AttriCtrl. A total of 10 participants evaluate 100 such comparisons, covering all four attributes and diverse intensity ranges. As summarized in Table 1, AttriCtrl significantly outperforms all other baselines. This demon-

Table 1: User study results. Percentage of times each method was selected as producing the most natural and coherent attribute progression across varying intensity values.

Methods	Bright.	Detail	Realism	Safety	Avg
Prompt-C	7.06%	8.18%	7.27%	4.41%	6.73%
Kontext-C	2.94%	0.61%	0.61%	0.29%	1.11%
Prompt-N	0.59%	5.76%	4.85%	0.59%	2.95%
Kontext-N	0.00%	1.52%	1.52%	0.00%	0.76%
Tie	2.94%	3.33%	1.82%	2.94%	2.76%
Ours	86.47%	80.61%	83.94%	91.76%	85.70%

Table 2: We measure control accuracy using the average absolute difference (AvgDiff ↓) between the target and result attribute intensity values.

Methods	Bright.	Detail	Realism	Safety
Prompt-N	0.279	0.414	0.271	0.329
Kontext-N	0.274	0.411	0.267	0.325
Ours	0.206	0.360	0.251	0.300

strates that AttriCtrl produces more semantically coherent transitions across intensity values, aligning better with human perception of precise and controllable editing.

Quantitative Evaluations

To quantitatively assess the effectiveness of aesthetic attribute control, we compare our method with two baselines from the numerical textual control paradigm: Prompt-N and Kontext-N. We randomly sample 5,440 high-quality prompts from DiffusionDB (Wang et al. 2022), covering a diverse set of visual scenarios. For each prompt, a target attribute intensity value $v_{\text{target}} \in [0, 1]$ is sampled, and an image is generated accordingly. We then compute the raw attribute value from the generated image and normalize it to $v_{\text{result}} \in [0, 1]$ using a quantile-based mapping derived from the training set. This mapping is obtained by identifying the closest match in the training distribution and retrieving its corresponding normalized intensity. Control accuracy is measured by the average absolute difference between the target and achieved attribute values:
$$\text{AvgDiff} = \frac{1}{N} \sum_{i=1}^N |v_{\text{target}}^{(i)} - v_{\text{result}}^{(i)}|$$
. As shown in Table 2, our method consistently achieves the lowest AvgDiff across all attributes, significantly outperforming both prompt-based and post-editing baselines, thereby demonstrating superior control precision.

To further evaluate safety intensity control, we compare our method with several state-of-the-art content moderation approaches: SLD (Schramowski et al. 2023), ESD (Gandikota et al. 2023), SPM (Lyu et al. 2024), and FMN (Zhang et al. 2024). We adopt the I2P prompt dataset (Schramowski et al. 2023) for evaluation and set the target safety intensity of AttriCtrl to 1, aiming for maximum suppression of unsafe content. The removal rate (RR) is calculated as:
$$\text{RR} = \frac{n_o - n_s}{n_o}$$
, where n_o is the number of unsafe images generated by the base model, and n_s is the number of unsafe outputs remaining after applying the safety control method. A higher RR indicates stronger suppres-

sion of harmful content. As reported in Appendix, AttriCtrl achieves the highest RR among all compared methods, demonstrating state-of-the-art safety controllability.

Applications of AttriCtrl

As illustrated in Figure 6, we integrate AttriCtrl with ControlNet (Zhang, Rao, and Agrawala 2023) by leveraging depth and canny maps as structural guidance to preserve global composition, while simultaneously modulating the brightness attribute. With content and layout held constant, our method enables smooth transitions in lighting, demonstrating the compatibility of AttriCtrl with existing conditional control frameworks. We further apply AttriCtrl to the InfiniteYou (Jiang et al. 2025) framework for personalized face generation. By fixing the identity embedding to preserve facial consistency, we modulate the brightness attributes. Results indicate that AttriCtrl enables fine-grained aesthetic control without compromising identity fidelity.

Conclusion

In this paper, we introduce AttriCtrl, a plug-and-play framework for fine-grained, multi-attribute control in diffusion models. By encoding normalized aesthetic values into learnable representations, our approach enables precise and continuous modulation of attributes such as brightness, detail, realism, and safety. Experimental results demonstrate that AttriCtrl outperforms both prompt-based and editing-based baselines in control accuracy and visual quality, with strong user preference. Moreover, it generalizes effectively to complex scenarios, including joint attribute control, safety enhancement, and integration with other control frameworks. AttriCtrl offers a flexible and scalable solution for more controllable and responsible image generation.

References

- Batifol, S.; Blattmann, A.; Boesel, F.; Consul, S.; Diagne, C.; Dockhorn, T.; English, J.; English, Z.; Esser, P.; Kullal, S.; et al. 2025. FLUX. 1 Kontext: Flow Matching for In-Context Image Generation and Editing in Latent Space. *arXiv e-prints*, arXiv-2506.
- Brooks, T.; Holynski, A.; and Efros, A. A. 2023. Instruct-pix2pix: Learning to follow image editing instructions. In *Proceedings of the IEEE/CVF conference on computer vision and pattern recognition*, 18392–18402.
- Celona, L.; Leonardi, M.; Napoletano, P.; and Rozza, A. 2022. Composition and style attributes guided image aesthetic assessment. *IEEE Transactions on Image Processing*, 31: 5009–5024.
- CompVis. 2022. stable-diffusion-safety-checker, <https://huggingface.co/CompVis/stable-diffusion-safety-checker>.
- Fan, Y.; Watkins, O.; Du, Y.; Liu, H.; Ryu, M.; Boutilier, C.; Abbeel, P.; Ghavamzadeh, M.; Lee, K.; and Lee, K. 2023. Dpok: Reinforcement learning for fine-tuning text-to-image diffusion models. *Advances in Neural Information Processing Systems*, 36: 79858–79885.
- Gandikota, R.; Materzynska, J.; Fiotto-Kaufman, J.; and Bau, D. 2023. Erasing concepts from diffusion models. In *Proceedings of the IEEE/CVF International Conference on Computer Vision*, 2426–2436.
- Hertz, A.; Mokady, R.; Tenenbaum, J.; Aberman, K.; Pritch, Y.; and Cohen-Or, D. 2022. Prompt-to-prompt image editing with cross attention control. *arXiv preprint arXiv:2208.01626*.
- Ho, J.; Jain, A.; and Abbeel, P. 2020. Denoising diffusion probabilistic models. *Advances in neural information processing systems*, 33: 6840–6851.
- Jiang, L.; Yan, Q.; Jia, Y.; Liu, Z.; Kang, H.; and Lu, X. 2025. InfiniteYou: Flexible photo recrafting while preserving your identity. *arXiv preprint arXiv:2503.16418*.
- Kirstain, Y.; Polyak, A.; Singer, U.; Matiana, S.; Penna, J.; and Levy, O. 2023. Pick-a-pic: An open dataset of user preferences for text-to-image generation. *Advances in neural information processing systems*, 36: 36652–36663.
- Kumari, N.; Zhang, B.; Zhang, R.; Shechtman, E.; and Zhu, J.-Y. 2023. Multi-concept customization of text-to-image diffusion. In *Proceedings of the IEEE/CVF conference on computer vision and pattern recognition*, 1931–1941.
- Labs, B. F. 2025. FLUX, <https://github.com/black-forest-labs/flux>.
- Liang, Y.; He, J.; Li, G.; Li, P.; Klimovskiy, A.; Carolan, N.; Sun, J.; Pont-Tuset, J.; Young, S.; Yang, F.; et al. 2024. Rich human feedback for text-to-image generation. In *Proceedings of the IEEE/CVF Conference on Computer Vision and Pattern Recognition*, 19401–19411.
- Lyu, M.; Yang, Y.; Hong, H.; Chen, H.; Jin, X.; He, Y.; Xue, H.; Han, J.; and Ding, G. 2024. One-dimensional Adapter to Rule Them All: Concepts Diffusion Models and Erasing Applications. In *Proceedings of the IEEE/CVF Conference on Computer Vision and Pattern Recognition*, 7559–7568.
- Meng, C.; He, Y.; Song, Y.; Song, J.; Wu, J.; Zhu, J.-Y.; and Ermon, S. 2021. Sdedit: Guided image synthesis and editing with stochastic differential equations. *arXiv preprint arXiv:2108.01073*.
- Mou, C.; Wang, X.; Xie, L.; Wu, Y.; Zhang, J.; Qi, Z.; and Shan, Y. 2024. T2i-adapter: Learning adapters to dig out more controllable ability for text-to-image diffusion models. In *Proceedings of the AAAI conference on artificial intelligence*, volume 38, 4296–4304.
- Nichol, A.; Dhariwal, P.; Ramesh, A.; Shyam, P.; Mishkin, P.; McGrew, B.; Sutskever, I.; and Chen, M. 2021. Glide: Towards photorealistic image generation and editing with text-guided diffusion models. *arXiv preprint arXiv:2112.10741*.
- openai. 2022. clip-vit-large-patch14, <https://huggingface.co/openai/clip-vit-large-patch14>.
- Podell, D.; English, Z.; Lacey, K.; Blattmann, A.; Dockhorn, T.; Müller, J.; Penna, J.; and Rombach, R. 2023. Sdxl: Improving latent diffusion models for high-resolution image synthesis. *arXiv preprint arXiv:2307.01952*.
- Radford, A.; Kim, J. W.; Hallacy, C.; Ramesh, A.; Goh, G.; Agarwal, S.; Sastry, G.; Askell, A.; Mishkin, P.; Clark, J.;

- et al. 2021. Learning transferable visual models from natural language supervision. In *International conference on machine learning*, 8748–8763. Pmlr.
- Raffel, C.; Shazeer, N.; Roberts, A.; Lee, K.; Narang, S.; Matena, M.; Zhou, Y.; Li, W.; and Liu, P. J. 2020. Exploring the limits of transfer learning with a unified text-to-text transformer. *Journal of machine learning research*, 21(140): 1–67.
- Ramesh, A.; Dhariwal, P.; Nichol, A.; Chu, C.; and Chen, M. 2022. Hierarchical text-conditional image generation with clip latents. *arXiv preprint arXiv:2204.06125*, 1(2): 3.
- Ramesh, A.; Pavlov, M.; Goh, G.; Gray, S.; Voss, C.; Radford, A.; Chen, M.; and Sutskever, I. 2021. Zero-shot text-to-image generation. In *International conference on machine learning*, 8821–8831. Pmlr.
- Rombach, R.; Blattmann, A.; Lorenz, D.; Esser, P.; and Ommer, B. 2022. High-resolution image synthesis with latent diffusion models. In *Proceedings of the IEEE/CVF conference on computer vision and pattern recognition*, 10684–10695.
- Ruiz, N.; Li, Y.; Jampani, V.; Pritch, Y.; Rubinstein, M.; and Aberman, K. 2023. Dreambooth: Fine tuning text-to-image diffusion models for subject-driven generation. In *Proceedings of the IEEE/CVF conference on computer vision and pattern recognition*, 22500–22510.
- Schramowski, P.; Brack, M.; Deiseroth, B.; and Kersting, K. 2023. Safe latent diffusion: Mitigating inappropriate degeneration in diffusion models. In *Proceedings of the IEEE/CVF Conference on Computer Vision and Pattern Recognition*, 22522–22531.
- Schuhmann, C.; Beaumont, R.; Vencu, R.; Gordon, C.; Wightman, R.; Cherti, M.; Coombes, T.; Katta, A.; Mullis, C.; Wortsman, M.; et al. 2022. Laion-5b: An open large-scale dataset for training next generation image-text models. *Advances in neural information processing systems*, 35: 25278–25294.
- Sheynin, S.; Polyak, A.; Singer, U.; Kirstain, Y.; Zohar, A.; Ashual, O.; Parikh, D.; and Taigman, Y. 2024. Emu edit: Precise image editing via recognition and generation tasks. In *Proceedings of the IEEE/CVF Conference on Computer Vision and Pattern Recognition*, 8871–8879.
- Si, C.; Huang, Z.; Jiang, Y.; and Liu, Z. 2024. Freeu: Free lunch in diffusion u-net. In *Proceedings of the IEEE/CVF Conference on Computer Vision and Pattern Recognition*, 4733–4743.
- Sohl-Dickstein, J.; Weiss, E.; Maheswaranathan, N.; and Ganguli, S. 2015. Deep unsupervised learning using nonequilibrium thermodynamics. In *International conference on machine learning*, 2256–2265. pmlr.
- Tsai, Y.-L.; Hsu, C.-Y.; Xie, C.; Lin, C.-H.; Chen, J.-Y.; Li, B.; Chen, P.-Y.; Yu, C.-M.; and Huang, C.-Y. 2023. Ring-a-bell! how reliable are concept removal methods for diffusion models? *arXiv preprint arXiv:2310.10012*.
- Voynov, A.; Aberman, K.; and Cohen-Or, D. 2023. Sketch-guided text-to-image diffusion models. In *ACM SIGGRAPH 2023 conference proceedings*, 1–11.
- Voynov, A.; Chu, Q.; Cohen-Or, D.; and Aberman, K. 2023. p+: Extended textual conditioning in text-to-image generation. *arXiv preprint arXiv:2303.09522*.
- Wallace, B.; Dang, M.; Rafailov, R.; Zhou, L.; Lou, A.; Purushwalkam, S.; Ermon, S.; Xiong, C.; Joty, S.; and Naik, N. 2024. Diffusion model alignment using direct preference optimization. In *Proceedings of the IEEE/CVF Conference on Computer Vision and Pattern Recognition*, 8228–8238.
- Wang, Z. J.; Montoya, E.; Munechika, D.; Yang, H.; Hoover, B.; and Chau, D. H. 2022. Diffusiondb: A large-scale prompt gallery dataset for text-to-image generative models. *arXiv preprint arXiv:2210.14896*.
- Wu, S.; Ding, F.; Huang, M.; Liu, W.; and He, Q. 2024. VMix: Improving Text-to-Image Diffusion Model with Cross-Attention Mixing Control. *arXiv preprint arXiv:2412.20800*.
- Wu, X.; Hao, Y.; Sun, K.; Chen, Y.; Zhu, F.; Zhao, R.; and Li, H. 2023. Human preference score v2: A solid benchmark for evaluating human preferences of text-to-image synthesis. *arXiv preprint arXiv:2306.09341*.
- Xiao, G.; Yin, T.; Freeman, W. T.; Durand, F.; and Han, S. 2025. Fastcomposer: Tuning-free multi-subject image generation with localized attention. *International Journal of Computer Vision*, 133(3): 1175–1194.
- Ye, H.; Zhang, J.; Liu, S.; Han, X.; and Yang, W. 2023. Ip-adapter: Text compatible image prompt adapter for text-to-image diffusion models. *arXiv preprint arXiv:2308.06721*.
- Zhang, G.; Wang, K.; Xu, X.; Wang, Z.; and Shi, H. 2024. Forget-me-not: Learning to forget in text-to-image diffusion models. In *Proceedings of the IEEE/CVF Conference on Computer Vision and Pattern Recognition*, 1755–1764.
- Zhang, H.; Duan, Z.; Wang, X.; Chen, Y.; and Zhang, Y. 2025. Eligen: Entity-level controlled image generation with regional attention. *arXiv preprint arXiv:2501.01097*.
- Zhang, L.; Rao, A.; and Agrawala, M. 2023. Adding conditional control to text-to-image diffusion models. In *Proceedings of the IEEE/CVF international conference on computer vision*, 3836–3847.